JOURNAL OF MATERIALS SCIENCE **36** (2001) 1349–1361

Real-time small angle X-ray scattering study of two-stage melt crystallization of PEEK

G. GEORGIEV, P. S. DAI, E. OYEBODE, P. CEBE*
Department of Physics and Astronomy, Tufts University, Medford, MA 02155, USA
E-mail: peggy@cebe.phy.tufts.edu

M. CAPEL
Argonne National Laboratory, 9700 S. Cass Av., Bldg. 432, E004, Argonne, IL 60439, USA

We report a study of dual stage crystallization and subsequent melting of Poly(etherether ketone) (PEEK) and an 80/20 blend with Poly(etherimide) (PEI) using differential scanning calorimetry (DSC) and real-time small angle X-ray scattering (SAXS). The treatment scheme involves annealing/crystallization at T_1 followed by annealing/crystallization at T_2, where either $T_1 < T_2$ or $T_1 > T_2$. The holding time during isothermal melt treatment was varied. DSC studies show there exist two endotherms when $T_1 < T_2$, and three endotherms when $T_1 > T_2$, for both PEEK and PEEK/PEI blend. Dual populations of crystals form during the first stage regardless whether $T_1 < T_2$ or $T_1 > T_2$. In the high-to-low temperature sequence, holding at the second stage causes an additional third population of crystals to grow, creating a third endotherm. As the first stage holding time increases, space available for the growth of additional crystals decreases, and the amount of crystals formed during the second stage decreases. During melting, the average long period increases while the linear stack crystallinity decreases continuously. The average crystal thickness also first increases, as the least perfect, thinnest crystals melt. Eventually, the crystal thickness levels off and begins to decline with increasing temperature. Melting of the thickest, most perfect crystals occurs most probably from the surfaces accounting for the roll-off and decrease in crystal thickness during the final stages of melting.

1. Introduction

The knowledge of the structure formation of crystalline polymers is very significant for many areas of contemporary science, e.g., physics, chemistry, materials science, theory of complexity. The non-equilibrium processes of crystallization are just beginning to be explained by our physical scientists. The non-equilibrium thermodynamics, nonlinear dynamics, the theory of chaos and fractals, play a growing role in the explanation of the processes that we study. Our understanding of the non-equilibrium and nonlinear processes of crystallization depends on our ability to apply modern analytical tools, such as synchrotron X-ray scattering, to these problems.

One of the many important problems in polymer physics that can be studied by X-ray scattering is structure formation, and its relationship to observations of multiple endothermic peaks seen in high performance polymers. Assignment of scattering peaks to structural entities within the material, the relative perfection of the crystals, and the possibility of their reorganization, are all influenced by the melt processing history. With the advent of high intensity synchrotron sources of X-radiation, polymer scientists gain a research tool which, when used along with thermal analysis, provides structural information about the crystals during growth and subsequent melting.

The subject of our present study is Poly(etheretherketone), PEEK, which is an engineering thermoplastic polymer. It has a very high glass transition temperature (145°C) and crystal melting point (337°C–342°C) [1, 2] making it suitable for high performance engineering applications in aerospace, automotive and electronics industries. In nearly all thermal studies, isothermally crystallized PEEK shows dual endotherms [1–5]. Small angle X-ray scattering (SAXS) and thermal studies have been used to address the formation of this dual endothermic response which has been variously ascribed to insertion of later-forming lamellar crystals between previously formed lamellae [6, 7], existence of distinct dual crystal populations [2, 8, 9], or melting of crystals followed by immediate re-crystallization [10, 11].

In addition to questions about the crystals themselves, recently a debate has arisen about the amorphous phase, and whether all of the amorphous phase of PEEK polymer is located in interlamellar regions [7, 11], or alternatively whether most is located in "pockets" away from the crystalline lamellar stacks [10, 12]. The

* Author to whom all correspondence should be addressed.

interpretation of scattering from lamellar stacks varies depending upon whether such amorphous pockets are assumed to be formed. From Babinet's principle of reciprocity, the small angle X-ray scattering pattern would be identical if the amorphous and crystal phases were exchanged. Thus, there is an ambiguity in the assignment of phase when the intercrystalline distance, or long period, L, is measured. L can only be written as $L = l_1 + l_2$ ($l_1 \leq l_2$), were l_1 may be either the crystal or the amorphous phase. We have adopted the assignment that the shorter length, l_1, should be associated with the crystalline phase. This assignment is consistent with other work in PEEK [7, 13, 14] and with our own previous studies of polyphenylene sulfide [15], PPS, an engineering polymer sharing many similarities with PEEK.

Studies of the location and rigidity of the amorphous phase, and interpretation of the dual melting endotherms, have been undertaken by our group in homopolymers [3, 16–19] and blends [20, 21]. Here, we apply the dual-stage melt crystallization treatment developed for PPS [17] to PEEK and to its blend with PEI. PEEK has been shown to be miscible in its melt state with another, but completely uncrystallizable polymer, poly(etherimide), PEI [22, 23]. Upon cooling from the melt state, PEEK crystallizes resulting in phase separation of the two blend components [12, 22, 24–28]. The main effects of blending PEI with PEEK are increasing the crystallization half-time, upward shift of the glass transition temperature, and reduction in overall level of crystallinity depending upon blend composition. We present a study of single and dual-stage melt crystallization of PEEK and an 80/20 PEEK/PEI blend. Real-time SAXS was used to follow the development of structural parameters, such as long period and crystal thickness, during crystallization and melting of these materials. Motivation for the two-stage thermal treatment was to provide additional information about structure formation when crystals grow in an environment restricted by the existence of other crystals formed during the first stage of treatment.

2. Experimental section

PEEK homopolymer in pellet form was obtained from ICI Americas. Compression molding at 400°C followed by quenching into ice water was used to obtain amorphous films. Dr. B. Hsiao kindly provided the PEEK/PEI blend films of composition ratio 80/20. Small angle X-ray scattering intensities were recorded *in situ* during crystallization and melting. Experiments were performed at the Brookhaven National Synchrotron Light Source (NSLS) beamline X12B with samples encapsulated in Kapton^{TM} tape, and heated in a Mettler FP80 hot stage.

The SAXS system at NSLS was equipped with a two-dimensional position sensitive detector. The sample to detector distance was 172.7 cm and the X-ray wavelength was .154 nm. SAXS data were taken continuously during the isothermal periods, heating/cooling between stages, and final heating to 360°C. Each SAXS scan was collected for 30 sec. Since the samples were isotropic, circular integration of the scattered intensity, I, was used to increase the signal to noise ratio. The following corrections were made to the SAXS raw intensity: background subtraction, sample absorption, changes in incident beam intensity, and thermal density fluctuation correction from Is^4 vs. s^4 plot ($s = 2\sin\theta/\lambda$ where θ is the half scattering angle) [29]. Structural parameters were determined from the one dimensional electron density correlation function, $K(z)$, obtained by discrete Fourier analysis of the Lorentz corrected intensity [30]. $K(z)$ was determined from:

$$K(z) = \sum_{j=1}^{N} (4\pi I_{corr}) s^2 \omega_N^{(j-1)(z-1)} \quad (1)$$

where:

$$\omega_N = e^{-2\pi i/N} \quad (2)$$

is the Nth root of unity [31]. In Equation 1, z is the direction normal to the lamellar stacks; N is the number of actual data points; and I_{corr} is the intensity, corrected for background and thermal density fluctuations. Linear extrapolation from the beam stop region to $s = 0$ was used in the summation. The long period, L, scattering invariant, Q, linear stack crystallinity, χ_c, and crystal thickness, l_c, are determined from $K(z)$ according to the method of Strobl and Schneider [30]. This approach will be described more fully in the Results section. The amorphous layer thickness, l_a, is determined by $l_a = L - l_c$. As mentioned before, we select l_c so that $l_c < l_a$, in agreement with results of others on PEEK [7, 11, 13, 14, 27, 32] and with our own prior work in poly(phenylene sulfide) [15].

Dual stage crystallization was used to study the relative perfection of the crystals formed from the melt. Fig. 1 shows the treatment schemes for dual stage melt crystallization. The samples were heated to 375°C and were held there for three minutes so as to erase the crystals from previous treatments before cooling to the first stage crystallization temperature. Samples were cooled at 5°C/min to 310°C, or at higher than 20 °C/min.

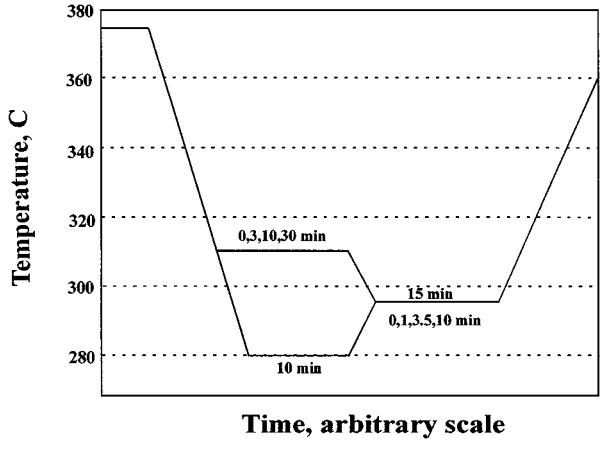

Figure 1 Thermal treatment scheme for PEEK and PEEK/PEI blends. Samples are initially heated to 375°C to melt, then cooled at 10°C/min to the first stage crystallization temperature (either 310°C or 280°C) and held for various times. The samples are then heated at 5°C/min to 295°C and held for various times before final heating at 5°C/min to 360°C.

TABLE I Treatment combinations for two-stage melt crystallization

	Temperature, °C	Time, min.
First Stage - High	310	0, 3, 10, 30
Second Stage - Low	295	15
First Stage - Low	280	10
Second Stage - High	295	0, 1, 3.5, 10

to 280°C. After a holding time at the first stage, samples were cooled from 310°C (or heated from 280°C) to the second stage temperature of 295°C at a rate of ±5°C/min. After a holding period at 295°C, the samples were heated at 5°C/min to 360°C. Table I shows the combination of temperatures and times used for the two-stage melt crystallization. The table shows that in the treatment scheme "high temperature to low" (i.e., $T_1 = 310°C > T_2 = 295°C$) the holding time at the first stage was varied. When the scheme was "low temperature to high" (i.e., $T_1 = 280°C < T_2 = 295°C$) the holding time at the second stage was varied.

When the first stage temperature is higher than the second stage (310°C–295°C), kinetics is slow enough in both PEEK and the PEEK/PEI blend [13] that little nucleation occurred before the sample equilibrated at 310°C. On the other hand, when the first stage temperature is lower than the second stage (280°C–295°C), both PEEK homopolymer and the 80/20 PEEK/PEI blend were already well-nucleated by the time the sample reached 280°C. To gain some information about when the nucleation begins, we performed studies at two cooling rates, and observed the first appearance of scattered intensity in the small angle X-ray pattern. At a relatively slow cooling rate of 5°C/min, the nucleation of crystals starts at temperature below 320°C for the homopolymer and below 315°C for the blend. Kinetics is slow at these temperatures and very little crystallinity develops by the time the first stage temperature, 310°C, is reached. At a cooling rate higher than 20°C/min. both the homopolymer and the blend start to nucleate at temperatures lower than 312°C. As a result of the faster kinetics at lower temperature, by the time the first stage temperature, 280°C, is reached, the spherulites have already impinged.

Thermal analysis was performed using a TA Instruments 2920 differential scanning calorimeter (DSC). Samples were treated to nearly the same experimental protocol used at the synchrotron, with exceptions noted when the DSC results are presented. Melting peak temperatures were calibrated using indium standard. Sample weight was around 8 mg. Nitrogen gas was used to purge the cell, at flow rate of 30 ml/min.

In this paper we use units for the temperature from the Celsius temperature scale. The conversion from degrees Celsius to degrees Kelvin is as follows:

$$T[\mathrm{K}] = T[^\circ\mathrm{C}] + 273.15$$

3. Results

3.1. Dual stage crystallization—low temperature to high

The DSC endothermic heat flow vs. temperature after four "low-to-high" thermal treatments is presented in Fig. 2a and b for PEEK and the 80/20 blend, respectively. All the samples were first annealed in the DSC for 10 min. at 280°C, followed by treatment at 295°C for 0 min. (curve a), 1 min. (curve b), 3.5 min. (curve c), and 10 min. (curve d). Prior to DSC scanning, all samples were first jumped down in temperature to 270°C, and the endothermic response recorded during heating from 270°C. The jump to 270°C was needed to resolve the small endotherm at 287°C, which otherwise was lost in the instrument stabilization period during the changeover from isothermal to non-isothermal scanning. In this regard (cooling to 270°C before scanning), the DSC treatment differs slightly from the real-time treatment of samples during SAXS studies.

The general features of the endotherms are similar for PEEK and for the 80/20 blends. All treatments result in dual endotherms. In the case of 0 min. at 295°C (curves a, in Fig. 2a and b) the lower endotherm occurs at about 287°C as a result of the first stage treatment at 280°C. When the holding time at 295°C is 1, 3.5, or 10 min., the lower endotherm shifts upward to about 302°C. The upper melting endotherm is barely affected by treatment at 295°C. The blend (Fig. 2b) shows broader endotherms, and the lower endotherm in the blend is smaller in area when compared to the homopolymer scans (Fig. 2a).

The Lorentz corrected intensity, Is^2, vs. scattering vector, s is shown in Fig. 3a for several treatments. In Fig. 3a, intensity at 295°C is compared for PEEK homopolymer (two higher intensity curves, 1 and 2) and 80/20 PEEK/PEI blend (two lower intensity curves, 3 and 4). Since the measurement temperatures are the same (295°C), no effects of thermal expansion appear in Fig. 3a. Two treatments are shown: 30 min. at 310°C followed by 15 min. at 295°C (curves 1 and 3); and, 10 min. at 280°C followed by 3.5 min. at 295°C (curves 2 and 4).

DSC mass fraction crystallinity, f_c, is listed in Table II for the four samples. f_c is greater for both PEEK and the blend after the high-to-low treatment (310°C–295°C) than after the low-to-high treatment (280°C–295°C). While f_c of PEEK and its blend is, within error, comparable for the high-to-low treatment, the homopolymer develops greater crystallinity than the blend after the low-to-high treatment. This is a result of the faster kinetics in the homopolymer [12], which causes more crystals to develop during cooling to 280°C. Conversion of f_c to a volume fraction basis was not performed, because the actual density of the amorphous phase at high temperature is not known. The correction is typically small, reducing f_c by about 0.02 at most.

Fig. 3b shows the correlation function, $K(z)$, for the conditions represented by Fig. 3a, curve 2 (PEEK at 295°C, after treatment at 280°C). The figure illustrates assignment of long period, L, SAXS invariant, Q_i, and the crystal thickness, l_c, using the method of Strobl and Schneider [30]. L is determined from the location of the first maximum in $K(z)$ past $K(0)$. l_c is found from the point of intersection of the baseline, $-A$, with an extrapolation of the linear portion of $K(z)$ at low z. The invariant of an ideal two-phase structure, Q_i, is found

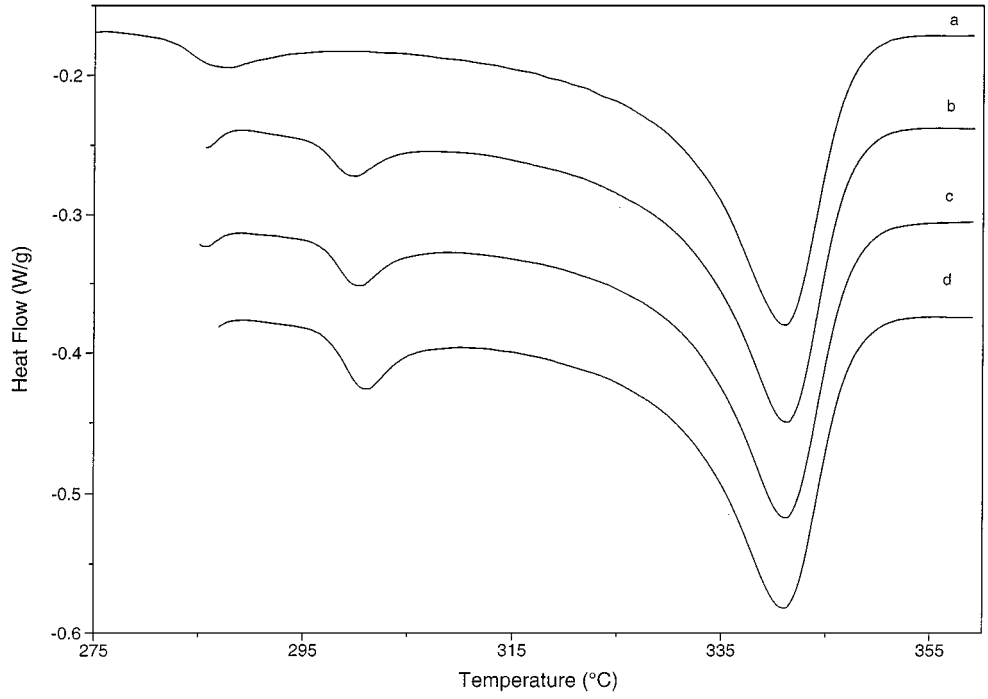

(a)

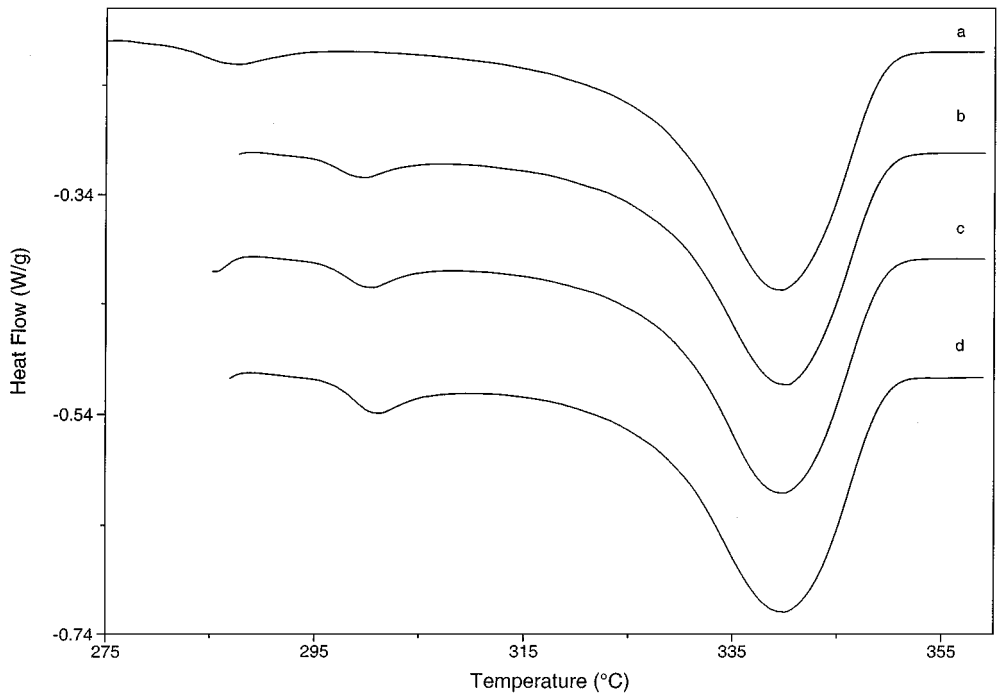

(b)

Figure 2 DSC endothermic heat flow vs. temperature for samples heated for 10 min. at 280°C followed by treatment at 295°C for 0 min. (curve a), 1 min. (curve b), 3.5 min. (curve c) and 10 min. (curve d). (a) PEEK; (b) 80/20 PEEK/PEI.

by extrapolation of the straight-line portion of $K(z)$ to its intersection at $z = 0$. Q is the measured value of $K(0)$ also shown for comparison. Departure of the measured Q from Q_i results from existence of an intermediate-density transition region of finite width at the boundary between the crystal and amorphous phases [30].

Values of L, l_c, χ_c (linear stack crystallinity, $\chi_c = l_c/L$), and Q_i are shown in Table II. The parameters L, l_c, and χ_c are greater after the 310°C–295°C treatment than after the 280°C–295°C treatment for both blend and homopolymer. The value of Q_i is greater by about a factor of five in the homopolymer compared to the blend.

Fig. 3c shows real-time Lorentz corrected intensity, Is^2, vs. scattering vector for PEEK homopolymer. The overall scheme is "low-to-high" with an initial treatment at 280°C followed by annealing at 295°C, then heating through melting. The curves from top to bottom represent different temperatures and times during the isothermal and non-isothermal periods, and these are listed in the legend on the right hand side of the plot frame. When the sample is fully melted, no Bragg peak can be detected.

As the holding time at 280°C increases, a weak shoulder grows up on the high-s side of the Bragg peak. An arrow marks the shoulder in Fig. 3c. After 10 min. at

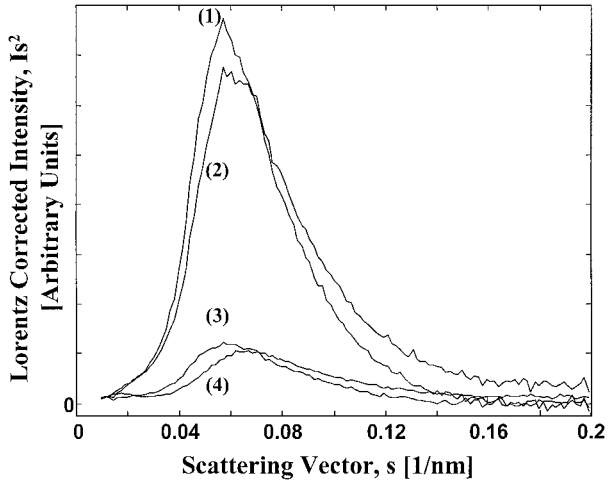

(a)

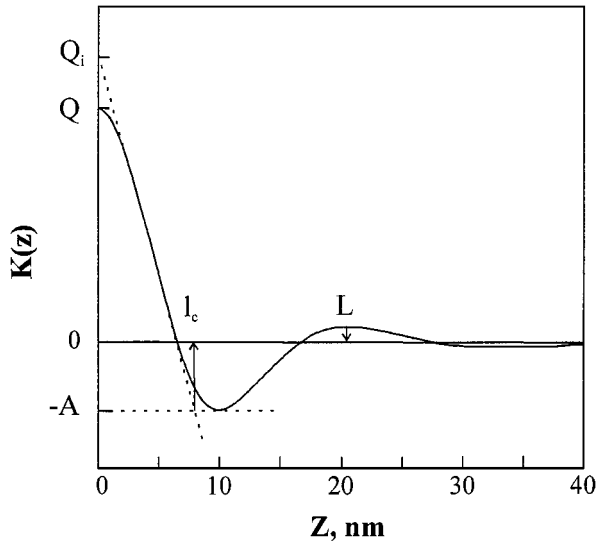

(b)

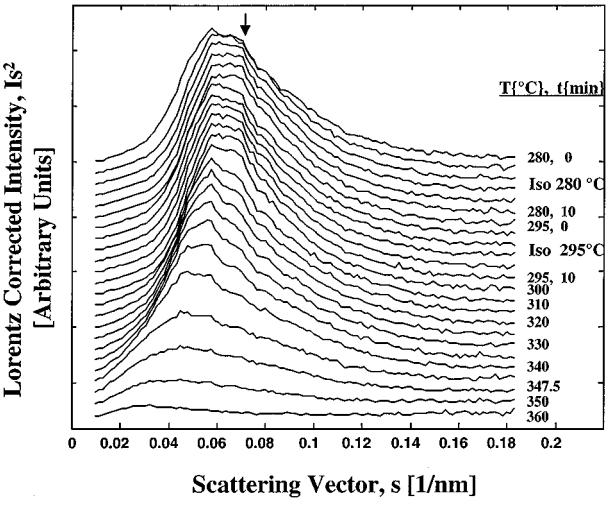

(c)

Figure 3 (a) Lorentz corrected intensity vs. scattering vector for PEEK (1, 2) and PEEK/PEI (3, 4) treated at 280°C, 10 min. (1, 3) or 310°C, 30 min. (2, 4). (b) One dimensional electron density correlation function, $K(z)$, from Equation. 1, for PEEK treated 10 min at 280°C, and then 3.5 min. at 295°C, showing determination of long period, L, crystal thickness, l_c, and scattering invariant, Q. (c) Lorentz corrected intensity vs. scattering vector for PEEK at a sequence of temperatures and times during "low-to-high" crystallization and melting. Temperatures and times are given in the legend. Appearance of a shoulder at high s (shown by an arrow) shows development of a population of less perfect crystals.

280°C the intensity in the shoulder is as large as intensity in the main Bragg peak. When the temperature first increases from 280°C to 295°C, the weak shoulder diminishes, and then increases once again as the holding time at 295°C increases. When the non-isothermal heating begins, and the temperature reaches 305°C, the intensity on the high s side decreases. As temperature increases, the Bragg maximum shifts to lower s.

3.2. Dual stage crystallization—high temperature to low

The DSC endothermic heat flows vs. temperature after four "high-to-low" thermal treatments is presented in Fig. 4a and b for PEEK and 80/20 blend, respectively. All the samples were crystallized at 310°C, but the times varied. Samples were held at 310°C for 0 min. (curve a), 3 min. (curve b), 10 min. (curve c), and 30 min. (curve d), followed by cooling to 295°C, and holding there for 15 min. After this second stage of treatment, the sample was jumped to 280°C, in order to resolve the lowest endotherm during subsequent DSC scanning to 360°C. When the sample receives only treatment at 295°C (0 min. at 310°C, curve a) dual endotherms are observed. Increasing the time of treatment at 310°C results in development of a middle endotherm, and a decrease of the area of the lowest endotherm with increased holding time at 310°C. The lowest endotherm of the triplet is the weakest, and can barely be seen in the blend, Fig. 4b. In both blend and homopolymer the lowest endotherm is largest when there is no pretreatment at 310°C, and decreases as the holding time at 310°C increases.

The middle endotherm, which arises only after treatment at 310°C, increases in area as the holding time at 310°C increases. The main melting endotherm, which peaks at about 340°C, is almost constant with crystallization time at 310°C. Melting is completed by 350°C. The location, shape, and total area of the small endotherms depend on the sample's prior thermal history, specifically on the isothermal holding times, given that all other parameters are held constant. In addition to the formation of the most perfect crystals (forming the high melting endotherm), we also observe the development of the less perfect populations of crystals during isothermal periods, which gives the melting peaks with lower melting temperature.

3.3. Structural parameters from SAXS

Fig. 5a–d shows the structural parameters, L and l_c, vs. time for PEEK homopolymer, determined by $K(z)$. The treatment shown is "low-to-high" and the following symbols pertain to all sections of the figure. The samples have 10 min at 280°C, followed by: 0 min. at 295°C (open circles), 1 min. at 295°C (crosses), 3.5 min. at 295°C (stars), and 10 min. at 295°C (solid line). The sample treated with no second stage treatment (open circles) actually had only 9 min. at 280°C (due to human error), and the first two data points shown are representative of non-isothermal cooling to 280°C, followed by 9 min. isothermal period. After the isothermal period,

TABLE II DSC crystallinity, f_c, and structural parameters from SAXS for PEEK and PEEK/PEI blends comparing two thermal treatments

PEEK/PEI	Thermal treatment	f_c[a] (±0.01)	L[b] (nm ±0.15)	l_c[b] (nm ±.02)	χ_c[c] (±0.01)	Q_i[d] (arb.)
100/0	310°C, 30 min. + 295°C, 15 min.	0.41	21.4	8.8	0.41	9.2$\underline{5}$
100/0	280°C, 10 min. + 295°C, 3.5 min.	0.37	20.3	7.6	0.38	8.9$\underline{7}$
80/20	310°C, 30 min. + 295°C, 15 min.	0.40	21.1	8.4	0.40	1.5
80/20	280°C, 10 min. + 295°C, 3.5 min.	0.34	20.3	7.1	0.35	1.2

[a] Mass fraction, determined by DSC from: (total endothermic area)/(130 J/g) [1].
[b] Determined from the correlation function (see Fig. 3b).
[c] Linear stack crystallinity, $\chi_c = l_c/L$.
[d] Determined from the correlation function (see Fig. 3b). SAXS intensity is not placed on an absolute scale, so the values of Q_i are relative. The third figure (underlined) is not significant, but is included to show the range.

this sample was directly heated to melt it. The other samples experience a heating ramp between the 280°C and 295°C stages, isothermal period at 295°C, and finally a second heating ramp to melt the sample. The heating ramp between stages is marked on the plot.

Fig. 5a shows L vs. time with all treatments superimposed, while b shows the L curves each separated by ~1 nm for clarity. The superimposed curves show that run-to-run variability was small (maximally .3 nm out of ~20 nm). Long period decreases during the isothermal holding time at 280°C. During the heating ramp from 280°C–295°C, L increases by about 1 nm. During holding at 295°C, L decreases very slightly. Upon subsequent heating to melt the sample, L increases in roughly two stages of differing slope. The change in slope to steeply rising occurs at about 335°C, just at the beginning of the major endotherm. When the temperature increases to 350°C, a Bragg peak can no longer be observed, and no long period can be calculated.

Fig. 5c and d shows lamellar thickness (crystal thickness) vs. time with all data superimposed (Fig. 5c) or separated for clarity by ~0.2 nm (Fig. 5d). Among the four runs, the variability in l_c during initial equilibration at 280°C is 0.05–0.1 nm. During the isothermal periods, and heating, variability is about .025 nm. The trends in l_c are similar, prior to final heating, to those seen for L. Viz., l_c decreases during the isothermal holding period at the first stage, increases (by ~0.1 nm) during heating from 280°C to 295°C, holds nearly steady during annealing at 295°C, then increases again during the first part of heating to melt the sample. The important difference in behavior between L and l_c is that L increases with continuously increasing slope throughout the melting, with steepest increase coming at the highest temperatures. l_c on the other hand, increases in the temperature range from 295–340°C, and then flattens as temperature increases further.

Fig. 6a and b shows the structural parameters, L and l_c, vs. time for PEEK homopolymer. The treatment shown is "high-to-low" and samples have variable holding times at the first stage temperature, 310°C. The following symbols pertain to all sections of the figure: treatment times at 310°C are 0 min. (open circles), 3 min. (crosses), 10 min. (stars), and 30 min. (dots). After the first stage, the samples were cooled to 295°C, held for 15 min., and then heated through melting. An arrow marks the start of the isothermal holding period at 295°C on each curve of Fig. 6a (long period, L) and b (crystal thickness, l_c).

Fig. 6a shows L vs. time with curves separated for clarity. The numerical scale on the ordinate is correct only for the sample (open circles) with no holding time at 310°C. Considering this sample first, we see that L decreases steadily during cooling to 295°C, and reaches about 21.8 nm before it starts increasing during final heating. The other three samples, with variable holding times at 310°C have several features in common. L drops steeply at first and then more slowly during the holding time at 310°C. The non-isothermal cooling to 295°C results in a step decrease in either L or l_c, just to the left of the arrow marking the arrival at 295°C. During the isothermal treatment at 295°C, L continues to decrease a little and then increases during final heating. As temperature increases from 295°C, L monotonically increases. The steepest increase occurs during the melting within the major endotherm. One of the curves, holding time at 310°C of 10 min. (stars), stops at a temperature of 325°C, while the others continue entirely through melting.

Fig. 6b shows the same treatments for l_c, with curves vertically displaced by about .2 nm. Scaling is correct only for the sample having no holding time at 310°C (open circles). For the sample which received no holding time at 310°C, crystal thickness decreases during the cooling to 295°C, and continues decreasing but with reduced slope during the 15 min. holding time at 295°C. During heating to melt the sample, l_c increases to a maximum value and then levels off and decreases. For the other three samples having variable holding times at the first stage, crystal thickness decreases during the isothermal treatment at 310°C. Cooling to 295°C results in further decrease in l_c. Holding at 295°C for 15 min. also causes l_c to decrease. The amount of the decrease in l_c at 295°C is affected by the amount of time at 310°C: the longer the holding time in the first stage, the smaller is the decrease in l_c during the second stage. Immediately upon the start of heating, l_c begins to increase, but with decreasing slope. When the temperature reaches 340°C, l_c begins to decrease.

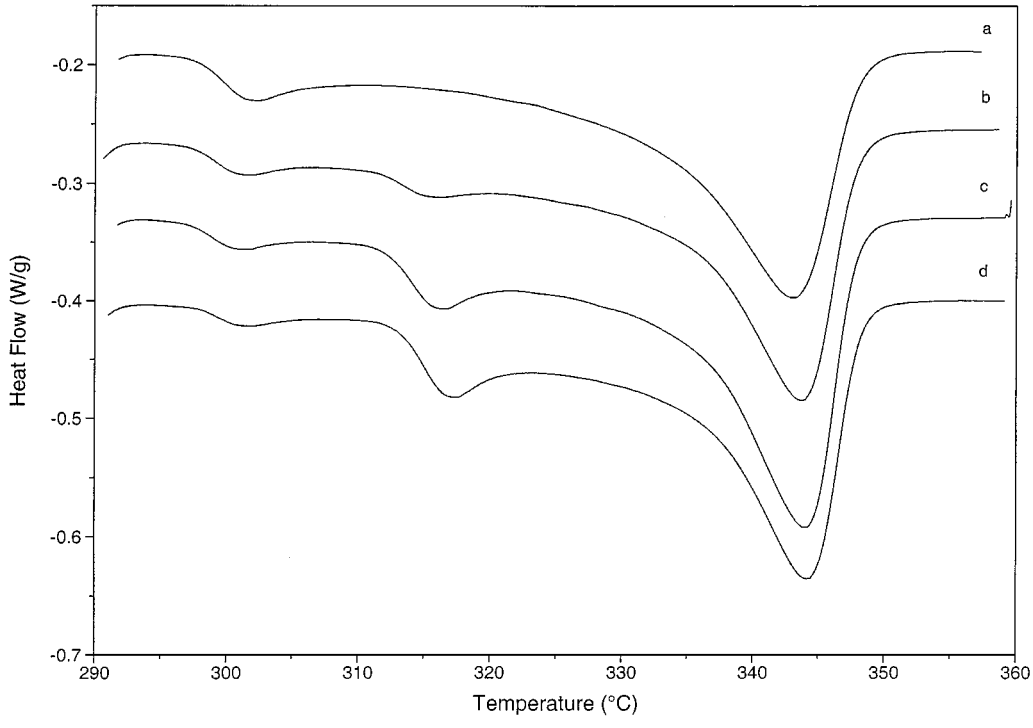

(a)

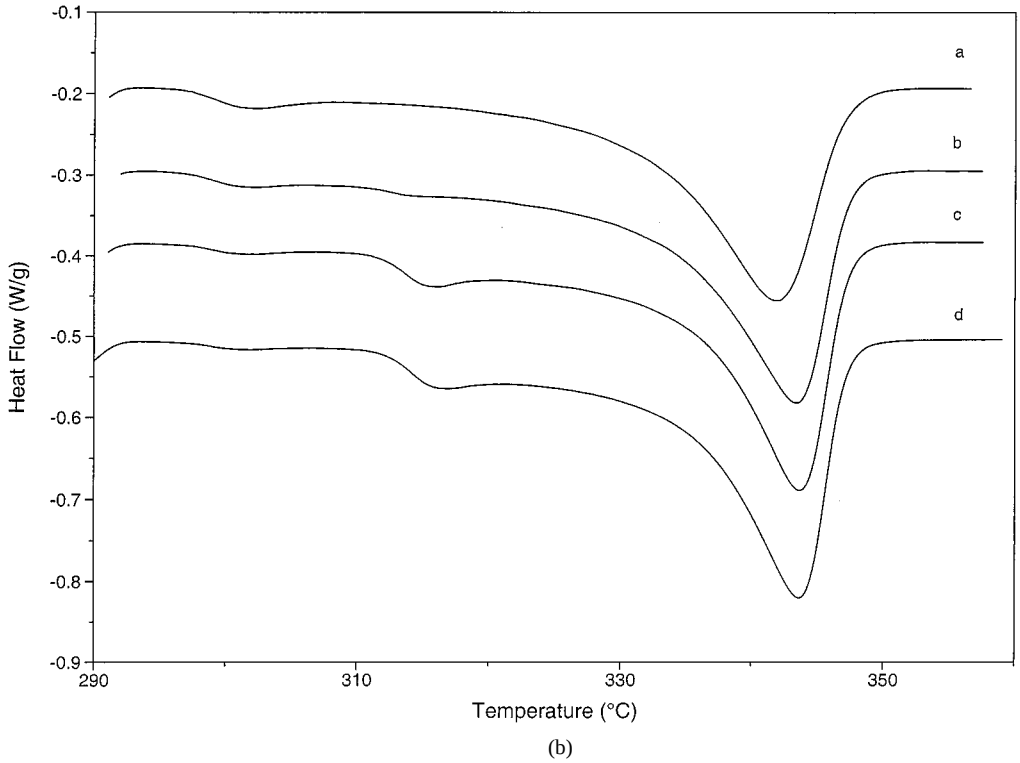

(b)

Figure 4 DSC endothermic heat flow vs. temperature for samples treated at 310°C for 0 min. (curve a), 3 min. (curve b), 10 min. (curve c) and 30 min. (curve d), followed by treatment at 295°C for 15 min. (a) PEEK; (b) 80/20 PEEK/PEI.

Fig. 7a–d shows the SAXS determined structural parameters for the 80/20 PEEK/PEI blend. Overall, the data for the blend samples was noisier than for the homopolymer, due to reduced scattered intensity in the blend. Curves are displaced vertically for clarity, and the upper curve (open circles) in each plot scales to the ordinate axis. Fig. 7a and b shows long period and crystal thickness, respectively, vs. time during dual stage "low-to-high" treatment. In Fig. 7a and b, the upper curves (open circles) show the treatment where the sample was held isothermally at 280°C and then melted. The lower curve (stars) shows the sample treated for 10 min. at 280°C followed by 3.5 min. at 295°C. The overall trends are the same in the blend as in the homopolymer: L and l_c both decrease slightly during holding at 280°C, and increase as temperature increases. For the sample treated at 295°C for 3.5 min, L and l_c both decrease again during the isothermal holding period at 295°C, and then increase immediately as the temperature increases during melting. L

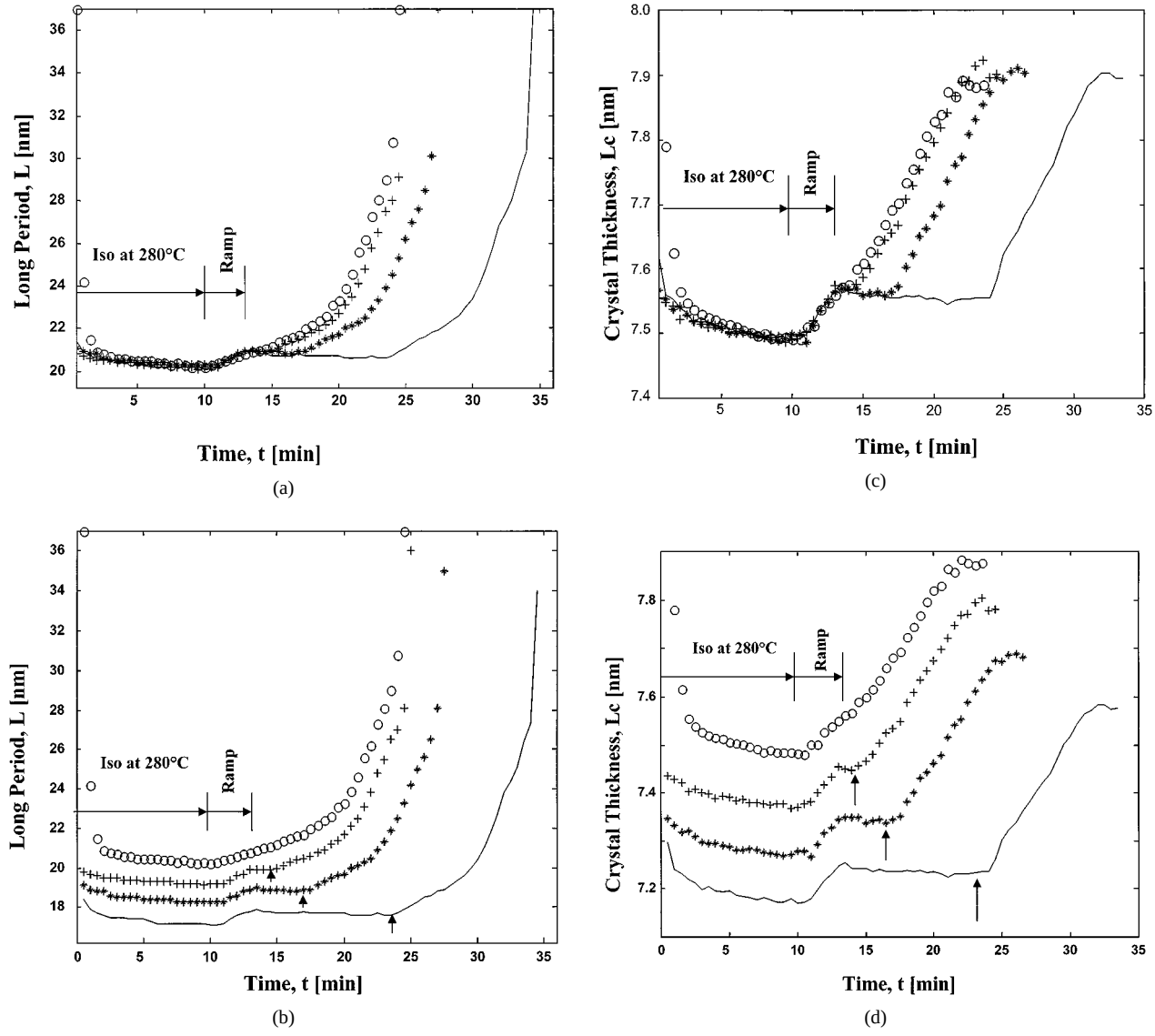

Figure 5 PEEK structural parameters for "low-to-high" two-stage melt treatment. Isothermal at 280°C followed by heat treatment at 295°C for: 0 min. (open circles), 1 min. (crosses), 3.5 min. (stars), and 10 min. (solid line), followed immediately by heating to melt the sample. (a) Long period vs. time; (b) Long period vs. time, with curves displaced vertically; (c) Lamella thickness vs. time; and (d) Lamella thickness vs. time, with curves displaced vertically. The arrows mark the end of the second isothermal period.

increases throughout melting, and the slope increases as temperature goes above 338°C.

Fig. 7c and d shows L and l_c, respectively, after treatment at 310°C for 0 min (open circles), 3 min (crosses), 10 min (stars) or 30 min (dots). Samples were cooled from 310°C, and the arrow on each curve shows the arrival at 295°C. L and l_c both decrease during the isothermal periods, and during cooling to 295°C. Then L increases dramatically throughout the melting range, while l_c first increases, then levels off or decreases slightly.

The linear stack crystallinity, χ_c, is shown in Fig. 8a and c for PEEK and Fig. 8b and d for the blend. Once again for clarity the curves have been displaced upwards vertically from a reference curve (open circles). An arrow marks the end of the isothermal period at 295°C. For the "low-to-high" treatments (Fig. 8a and b) the first stage treatment is the same for all curves, and the vertically shifted curves superimpose exactly on the reference curve during the first 10 minutes at 280°C. Crystallinity is relatively constant during the isothermal period at 280°C, increases very slowly during both heating to 295°C and holding at 295°C, then declines slowly as temperature increases from 295°C. The decrease is gentle up to 325°C, but crystallinity decreases rapidly as temperature increases through the upper melting endotherm region.

In the "high-to-low" treatments (Fig. 8c and d) average linear stack crystallinity increases rapidly during the first minute at 310°C for both homopolymer and blend. Crystallinity increases slightly throughout the isothermal period at 310°C. No change in crystallinity was seen during cooling to 295°C, and only a very slight increase was observed during the second stage isothermal period at 295°C. As shown in Table II, degree of crystallinity is 0.41 for PEEK and 0.40 for the blend at the end of the treatment sequence: 30 min. isothermal period at 310°C followed by 15 min. at 295°C. Crystallinity during final heating from 295°C followed the same trends as in the "low-to-high" thermal treatment.

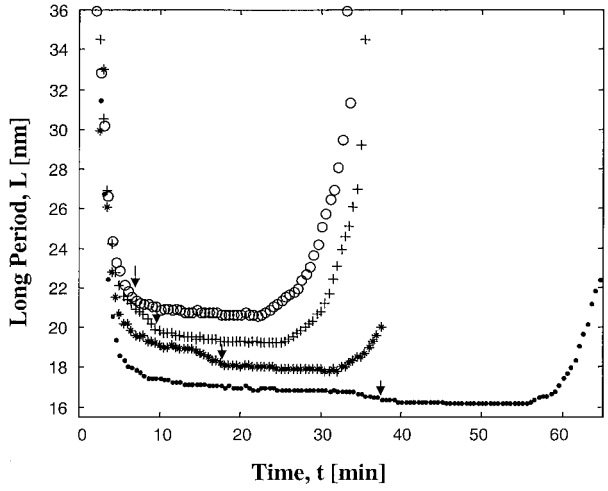

(a)

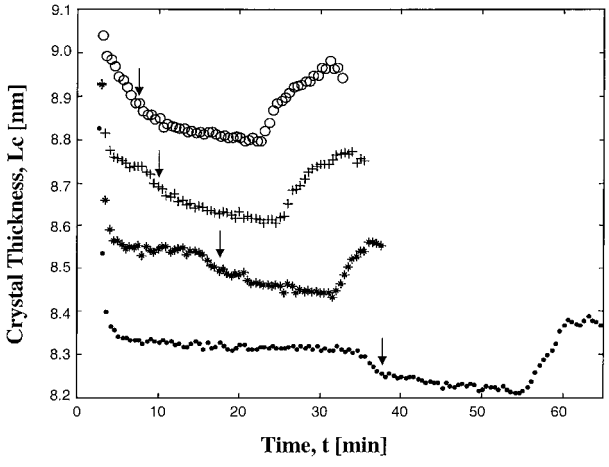

(b)

Figure 6 PEEK structural parameters for "high-to-low" two-stage melt treatment. Isothermal at 310°C for: 0 min. (open circles), 3 min. (crosses), 10 min. (stars), and 30 min. (dots), followed by heat treatment at 295°C for 15 min., and then heating to melt the sample. The arrows mark the start of the second stage isothermal treatment at 295°C. (a) Long period vs. time with curves displaced vertically; (b) Lamella thickness vs. time with curves displaced vertically.

4. Discussion

As shown in Fig. 3a, the intensity scattered by the blends is quite a bit smaller than that from the homopolymer. The difference in integrated areas is about a factor of five in this study. The integrated area is also called the scattering invariant, Q, and is given by [30]:

$$Q = \int_0^\infty 4\pi s^2 I_{\text{corr}}\, \text{ds} = \chi_s \chi_c (1 - \chi_c)(\rho_c - \rho_a)^2 \quad (3)$$

The integral is related to the spherulite filling fraction, χ_s, the linear stack crystallinity, χ_c, and the square of the difference in electron density between the crystals, ρ_c, and the amorphous phase, ρ_a. From Table II, the linear crystallinity, χ_c, in these samples is not sufficiently different to account for the very large differences in Q. Also from electron microscopy of blends of this composition [23, 24, 27], spherulites fill up the available volume completely so that χ_s is unity. Reduction in intensity in the blend is a result of a reduction in the electron density difference (i.e., scattering contrast) between the crystalline phase due to thermal expansion effects and mixing of interlamellar PEI.

4.1. Low-to-high thermal treatment

Our group has previously [16, 17] used thermal analysis to study effects of two-stage melt crystallization on the multiple melting of poly(phenylene sulfide). We proposed a model to explain multiple melting endotherms in PPS, treated according to one- or two-stage melt or cold crystallization [16, 17]. The key feature of this model is that multiple endotherms arise from different causes, depending upon the nature of the crystallization history. After crystallization from the glass at high undercooling (so-called "cold" crystallization), multiple endotherms are due to reorganization and/or recrystallization of imperfect crystals formed at low temperature. On the other hand, after melt crystallization at low undercooling, crystal morphology dominates the appearance of the melting endotherms. In other words, multiple distinct crystal populations, characterized by different levels of crystal perfection, are formed by the melt crystallization, leading to observation of multiple melting [16, 17].

Validity of the reorganization/recrystallization model for cold crystallization has been demonstrated for PEEK polymer through recent SAXS and DSC studies of heating or annealing of quenched PEEK [4, 14, 29]. Not as much work has been done on melt crystallization and the present work addresses the dual-stage thermal treatment uniquely, by considering both "low-to-high" and "high-to-low" temperature sequences.

From the DSC melting behavior (Fig. 2a and b) dual endotherms are always observed after two-stage melt crystallization from "low-to-high" temperature. The second stage treatment at 295°C, being at a temperature higher than that of the first stage minor endotherm, "erases" the first minor endotherm. In its place there appears a second, larger minor endotherm at still higher temperature, about 5–8 degrees above 295°C. The longer the holding time at 295°C, the larger is the area of the minor endotherm. The area and peak position of the major endotherm are nearly unaffected by the second stage thermal treatment. Similar behavior is seen for PEEK and for the 80/20 PEEK/PEI blend.

SAXS results (Fig. 3c) for the "low-to-high" treatment show that there is a small, but reproducible, change in intensity at higher s (referring to crystals having smaller average long periods). As the holding time during the first stage increases, intensity grows in a shoulder at higher s. Upon heating from 280°C to 295°C, through the first minor endotherm, the shoulder intensity drops, and then rises again during the second stage isothermal holding at 295°C. These small changes in SAXS intensity combined with the DSC endothermic behavior allow the conclusion that the minor endotherm represents melting of a population of less perfect crystals, which recrystallize and are able to become more perfected during the second stage holding time.

Fig. 3c shows that the long period of the crystals, corresponding to the characteristic melting endotherm for PEEK at 345°C, form in the first stages of the period

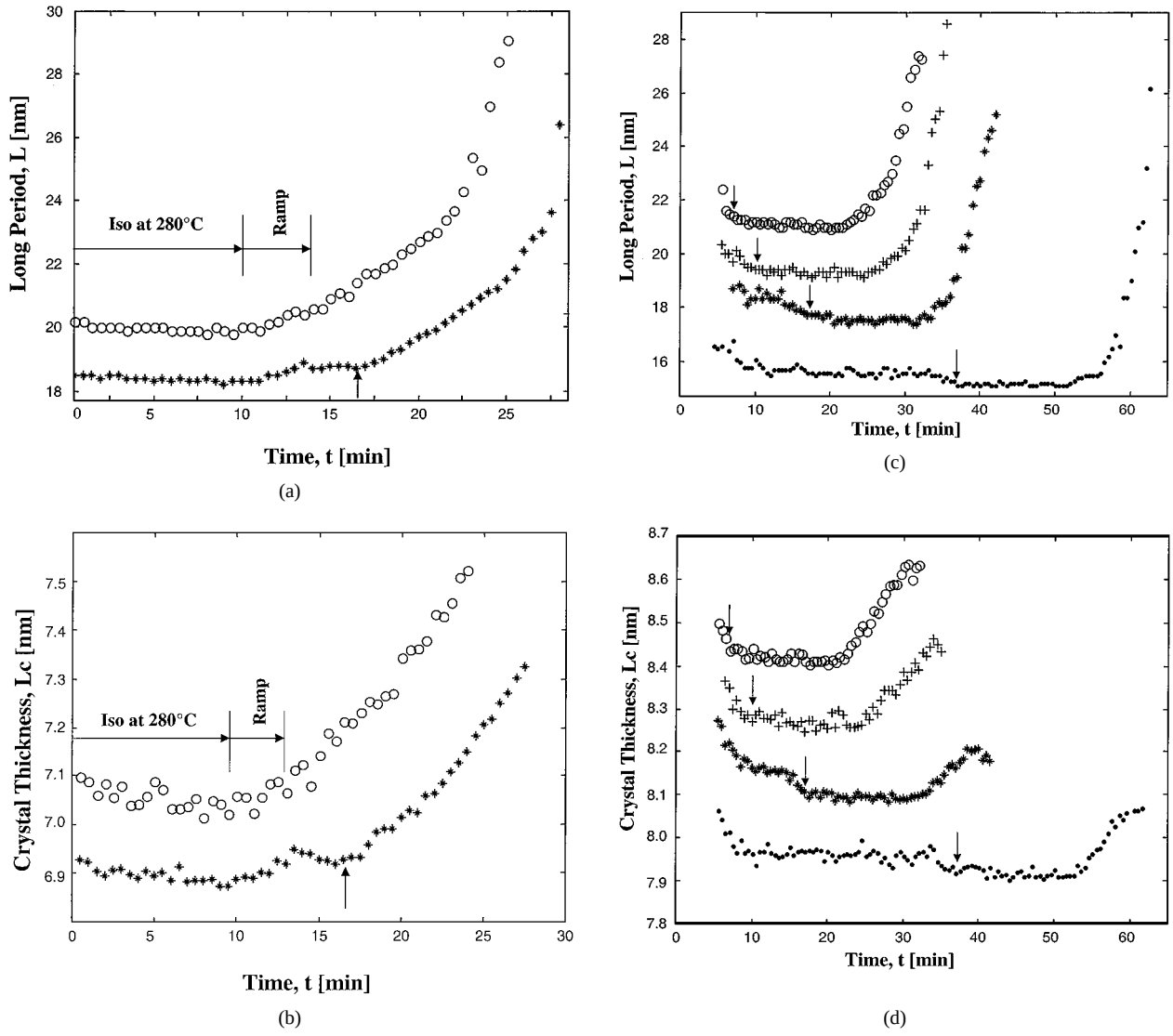

Figure 7 PEEK/PEI structural parameters for two-stage melt treatment: (a) Long period vs. time with curves displaced vertically; (b) Lamella thickness vs. time with curves displaced vertically. For (a) and (b): Isothermal at 280°C for 10 min., then 0 min. at 295°C (open circles) and 3.5 min. at 295°C (stars) followed by heating to melt. The arrows on Fig. 7a and b mark the end of the second stage isothermal treatment at 295°C. (c) Long period vs. time with curves displaced vertically; (c) Lamella thickness vs. time with curves displaced vertically. For (c) and (d): Isothermal at 310°C for 0 min. (open circles), 3 min. (crosses), 10 min. (stars) and 30 min. (dots), followed by 15 min. at 295°C and heating to melt. The arrows on Fig. 7c and d mark the start of the second stage isothermal treatment at 295°C.

prior to equilibration at 280°C, and then the second population with lower long period (intensity at higher s) starts to form. One possible explanation is that the main population of the crystals melting at 345°C is forming in an unconstrained molten environment during cooling to 280°C, and is independent of the temperature at which the crystals are formed. Once these crystals are formed, the second population corresponding to the given crystallization temperature, grows in a highly constrained environment, creating crystals which are less perfect and melt at lower temperature.

Perfection of crystals is seen as an increase of the intensity of the population scattering at higher s, while the intensity of the population scattering at lower s stays constant. During heating from below to above the minor endotherm, we see rapid decrease of the intensity of the X-ray scattering corresponding to the population of crystals scattering in the shoulder. Another important observation is that after the sample is annealed at 295°C, the shoulder intensity is progressively restored (Fig. 3c). The population scattering at higher s remains longer before it disappears in the sample treated to the second stage of melt crystallization, compare to the sample crystallized with a single stage. This could be interpreted as an effect of continued perfection of the less perfect population, also reflected in the increased melting temperature of the smaller endotherm as the holding time at 295°C increases. In the corresponding DSC scans (Fig. 2) we see a shift in the peak temperature and increase in area of the lower melting endotherm with an increase of the annealing time at 295°C.

Not all of the increase in long period seen in the non-isothermal stage (for example, heating from 280°C to 295°C) can be ascribed to thermal expansion effects. Most of the increase in L seen during heating through the minor endotherm is due to melting of the imperfect population of crystals. The measured increase in L between 280°C and 295°C is about 1 nm (Fig. 5a). The change in long period, ΔL, can be written in terms

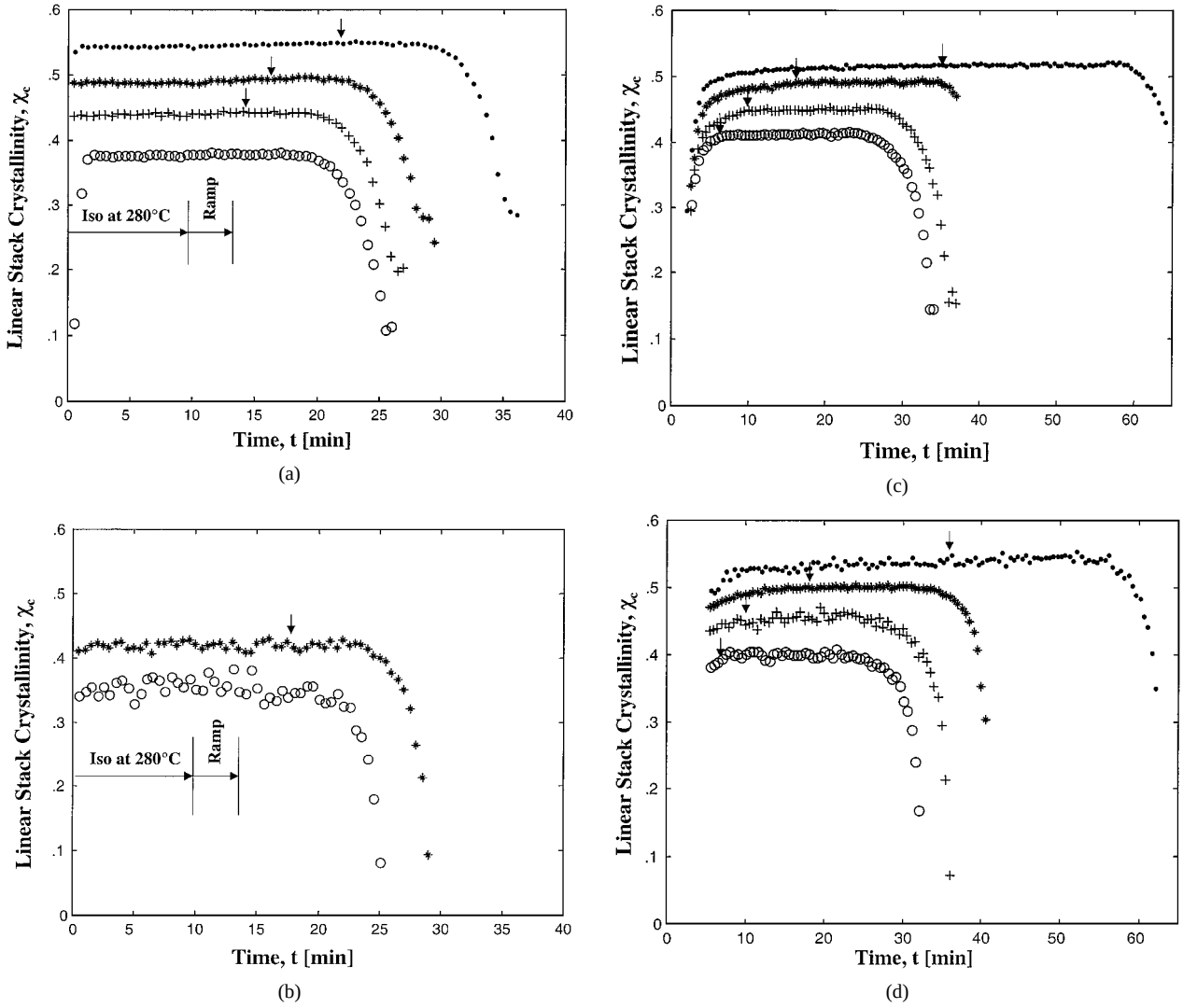

Figure 8 Linear stack crystallinity vs. time for various treatments. Isothermal at 280°C followed by heat treatment at 295°C for: 0 min. (open circles), 1 min. (crosses), 3.5 min. (stars), and 10 min. (dots), followed immediately by heating to melt the sample: (a) PEEK (b) 80/20 PEEK/PEI blend. Isothermal at 310°C for: 0 min. (open circles), 3 min. (crosses), 10 min. (stars), and 30 min. (dots), followed by heat treatment at 295°C for 15 min., and then heating to melt the sample: (c) PEEK (d) 80/20 PEEK/PEI blend. The arrows on Fig. 8a and b mark the end, and on Fig. 8c and d the start of the second stage isothermal treatment at 295°C.

of the change in temperature, ΔT, the long period at $T = 0$, $L(0)$, and the thermal expansion coefficient of the long period [35] as:

$$\Delta L = \Delta T L(0)\alpha^z \sim 0.1 \text{ nm} \qquad (4)$$

The calculation uses $\Delta T = 15°\text{C}$ and $\alpha^z = 4.3 \times 10^{-4}/°\text{C}$ [35]. Since we do not know $L(0)$, we replace that quantity with $L(280°\text{C}) \sim 20$ nm (from present data), which is surely larger. This results in a maximal estimate for the expected change in L caused by thermal expansion (or contraction) during heating (or cooling) between 280°C and 295°C. The actual measured change in L over this temperature interval is ten times greater than can be attributed to thermal expansion effects.

Similar trends after the "low-to-high" temperature treatment are observed for the blend (Fig. 7a and b) as for the pure PEEK. The blend long period and crystal thickness are smaller than for PEEK. This leads us to the idea that the amorphous PEI is located in-between the lamellae for our conditions of treatment, rather than in the interspherulitic or interfibrillar spaces, which is consistent with the observations of others [12, 27]. Also at the end of the isothermal period, the linear stack crystallinity, χ_c, shows only slightly higher value than f_c, the crystallinity derived from the DSC scans (see Table II). This supports our view that for our crystallization conditions there are no large amorphous pockets left outside the crystalline regions. In this respect we confirm the homogeneous model [27] in which crystal lamellae grow as space filling stacks. In agreement with the homogeneous model and the result that the crystallinity of all of our samples is less than 50%, we assign the smaller length as l_c. When we have the low-to-high isothermal period sequence, the small population of crystals, after melting at the small melting endotherm, re-crystallizes after this and forms a higher temperature melting population with slightly larger average lamellar thickness.

4.2. High-to-low thermal treatment

As the first stage holding time at 310°C increases, the area of the middle small peak increases (Fig. 4a) and its

melting temperature slightly increases. This indicates that a greater amount of material crystallizes during the 310°C isotherm, as the isothermal holding time increases. This is seen also in Fig. 8c, showing the slow but steady rise in χ_c during holding at 310°C. At the same time the material left to crystallize at 295°C is less and less with the increase of the first holding time. The effect of the 295°C treatment is to form a third, least perfect population of crystals melting in the lowest of the three endotherms seen in Fig. 4a. The size of this endotherm *decreases* as the first stage holding time increases. After dual stage crystallization with $T_1 > T_2$, the amount of space remaining for additional crystal growth at T_2 depends upon the holding time at T_1. The long period of crystals formed at T_2 is smaller than that formed at T_1 (Fig. 6a) due to growth in a now-restricted geometry.

Both L and l_c decrease during isothermal holding at 310°C, cooling to 295°C, and isothermal holding at 295°C. The size of the decrease during cooling is larger than can be accounted for by thermal contraction effects, but the change occurs with a constant l_c/L value (constant linear stack crystallinity, χ_c). Thus, additional crystals forming in the restricted spaces slightly reduce both the average long period and lamellar thickness but do not increase the linear stack crystallinity.

During the 295°C stage of the low-to-high treatment χ_c increases, but during the 295°C stage of the high-to-low treatment changes in χ_c are within the noise of the data. Heating from 280°C to 295°C melts some imperfect crystals, that crystallize once again at 295°C with higher l_c/L value. However, cooling from 310°C to 295°C causes additional crystal growth in a restricted geometry. The longer the holding time at 310°C, the less space available for additional crystals. After the high-to-low treatment it is much more difficult for the population of crystals formed at the lower annealing temperature to re-crystallize after it melts at the lowest endotherm. All of the material crystallizable at 310°C was already crystalline and the rest that was crystallized afterwards at 295°C was not previously crystallizable at 310°C.

4.3. Final melting

During the final melting sequence the lamellar thickness, l_c, first increases with nearly constant slope, and then rolls off (Figs. 5c and d, 6b and 7d). The increase begins immediately upon heating from the second stage treatment temperature. The initial increase is consistent with the progressive melting of the thinnest lamellae in the sample, which causes the average lamellar thickness steadily to increase. As the temperature increases to 325°C, within the major melting endotherm, L and l_c increase together. From 325°C to 340°C (the location of the major endotherm's peak), the DSC crystallinity is rapidly changing as crystals melt. By 340°C, less than half the original crystals remain in the sample. The linear stack crystallinity changes only a little in this temperature range: χ_c decreases from about 0.375 at 320°C to 0.35 at 340°C. Spherulites no longer fill the available volume and large regions devoid of crystals now are formed as temperature increases. The change in χ_s is the major contributor to the decrease in area under the scattering curves (Fig. 3c) above 345°C.

At temperatures above 340°C, we have remaining in the sample only the thickest, most perfected lamellae. During the last few minutes of melting, from 340°C to 345°C, the long period increases most steeply and the lamellar thickness rolls off. This roll-off is due to surface melting of these lamellae, which begins to reduce the average lamellar thickness. Eventually, the average lamellar thickness must decrease to zero, and we see a hint of this in the roll-off. However, above 345°C, there are only a few percent of crystals remaining in the sample, and the noise level is to too large for any structural parameters to be determined.

5. Conclusion

Small angle synchrotron X-ray scattering is an important tool for the study of real-time structure development in semicrystalline polymers. Changes in structural parameters such as long periodicity, lamellar thickness and linear crystallinity allow better understanding of primary and secondary crystallization processes which contribute to the dual, and even triple, endothermic response seen in PEEK polymer. Here, we used dual stage melt crystallization of PEEK and its 80/20 blend with PEI to study structure formation when crystals grow in an environment restricted by the existence of other crystals formed during the first stage of treatment.

During two-stage melt crystallization, dual populations of crystals form during the first stage regardless whether the treatment conditions are a low-to-high or high-to-low temperature sequence. During the first stage, the average long period and crystal thickness decrease, while linear stack crystallinity increases, with an increase in holding time.

In the low-to-high temperature sequence, heating to the second stage melts a population of least perfect crystals. A small intensity shoulder at high s decreases upon heating through the lower of the two endotherms, while the average long period, crystal thickness, and linear stack crystallinity all increase. During the holding at the second stage, additional crystals form. Scattered intensity increases in the high s shoulder, and average long period and crystal thickness decrease as some of the now-molten material recrystallizes.

In the high-to-low temperature sequence, cooling to, and holding at, the second stage causes the average long period and crystal thickness to decrease. Holding at the second stage causes an additional third population of crystals to grow, creating a third endotherm. As the first stage holding time increases, the middle small endotherm increases in area while the lowest small endotherm decreases. The amount of the crystals formed during the second stage decreases as the space available for their growth decreases.

During the melting sequence, the average long period increases steadily, gently at first and then with steep slope as temperature rises to the location of the peak in the major endotherm. The average crystal thickness also first increases, as the least perfect, thinnest crystals

melt. Eventually, the crystal thickness levels off and begins to decline with increasing temperature. We suggest that melting of the thickest, most perfect crystals occurs from the surfaces accounting for the roll-off and decrease in l_c.

Acknowledgments

The National Aeronautics and Space Administration, Grant NAG8-1167 supported this work.

References

1. D. J. BLUNDELL and B. N. OSBORN, *Polymer* (1981).
2. P. CEBE and S. D. HONG, *Polymer* **27** (1986) 1183.
3. P. CEBE, *J. Materials Science* **23** (1988) 3721.
4. D. BASSETT, R. OLLEY and A. AL RAHEIL, *Polymer* **29** (1988) 1745.
5. S. CHENG, Z. WU and B. WUNDERLICH, *Macromolecules* **20** (1987) 2802.
6. B. HSIAO, K. GARDNER, D. WU and B. CHU, *Polymer* **34** (1993) 3986.
7. A. JONAS, T. RUSSELL and D. YOON, *Macromolecules* **28** (1995) 8491.
8. B. HSIAO, B. SAUER, R. VERMA, H. ZACHMANN, S. SEIFERT, B. CHU and P. HARNEY, *ibid.* **28** (1995) 6931.
9. K. KRUGER and H. ZACHMANN, *ibid.* **26** (1993) 5202.
10. R. VERMA, V. VELIKOV, R. KANDER, H. MARAND, B. CHU and B. HSIAO, *Polymer* **37** (1996) 5357.
11. C. FOUGNIES, P. DAMMAN, D. VILLERS, M. DOSIERE and M. KOCH, *Macromolecules* **30** (1997) 1385.
12. B. HSIAO and B. SAUER, *J. Polym. Sci., Polym. Phys. Ed.* **31** (1993) 901.
13. C. FOUGNIES, P. DAMMAN, M. DOSIERE and M. KOCH, *Macromolecules* **30** (1997) 1392.
14. C. FOUGNIES, M. DOSIERE, M. KOCH and J. ROOVERS, *ibid.* **31** (1998) 6266.
15. S. X. LU, P. CEBE and M. CAPEL, *ibid.* **30** (20) (1997) 6243.
16. J. S. CHUNG and P. CEBE, *Polymer* **33** (11) (1992) 2312.
17. *Idem., ibid.* **33** (11) (1992) 2325.
18. P. HUO and P. CEBE, *Macromolecules* **25** (1992) 902.
19. S. X. LU and P. CEBE, *Polymer Comm.* **37** (21) (1996) 4857.
20. G. GEORGIEV, P. DAI, E. OYEBODE, P. CEBE and M. CAPEL, *MRS Proceedings*, Symposium on Applications of Synchrotron Radiation V (2000) 137.
21. P. HUO and P. CEBE, *Macromolecules* **26** (1993) 4275.
22. G. CREVECOEUR and G. GROENINCKX, *ibid.* **24** (1991) 1190.
23. H. CHEN and R. PORTER, *J. Polym. Sci., Polym. Phys. Ed.* **31** (1993) 1845.
24. S. HUDSON, D. DAVIS and A. LOVINGER, *Macromolecules* **25** (1992) 1759.
25. X. KONG, F. TENG, H. TANG, L. DONG and Z. FENG, *Polymer* **37** (1996) 1751.
26. B. HSIAO, R. VERMA and B. SAUER, *J. Macromol. Sci.-Phys.* **B37**(3) (1998) 365.
27. A. JONAS, D. IVANOV and D. YOON, *Macromolecules* **31** (1998) 5352.
28. C. LEE, T. OKADA, H. SAITO and T. INOUE, *Polymer* **38** (1997) 31.
29. O. GLATTER and O. KRATKY, "Small angle X-ray Scattering" (Academic Press Inc., NY, 1982).
30. G. R. STROBL and M. SCHNEIDER, *J. Polym. Sci., Polym. Phys. Ed.* **18** (1980) 1343.
31. *Matlab Reference Guide* (The Math Works, Inc.: Natick, MA, 1992) 182.
32. D. A. IVANOV, ROGER LEGRAS and ALAIN M. JONAS, *Macromolecules* **32** (1999) 1582.
33. Material Data Sheet for General Electric ULTEM (PEI), Boedeker Plastics (1999).
34. D. BLUNDELL and J. D'MELLO, *Polymer* **32** (1991) 304.
35. S. X. LU, P. CEBE and M. CAPEL, *Polymer* **37**(14) (1996) 2999.

Received 4 February
and accepted 2 August 2000